

APPENDIX A

Control regions for fakes

Comparisons of data with prediction for fakes control regions in the $H \rightarrow \tau\tau$ analysis are shown.

A.1 Same sign CR

A.2 MC SR

A.3 $W \rightarrow \ell\nu_\ell$ CR

A.4 QCD CR

A.5 $Z \rightarrow \ell\ell$ CR

A.6 top CR

A. CONTROL REGIONS FOR FAKES

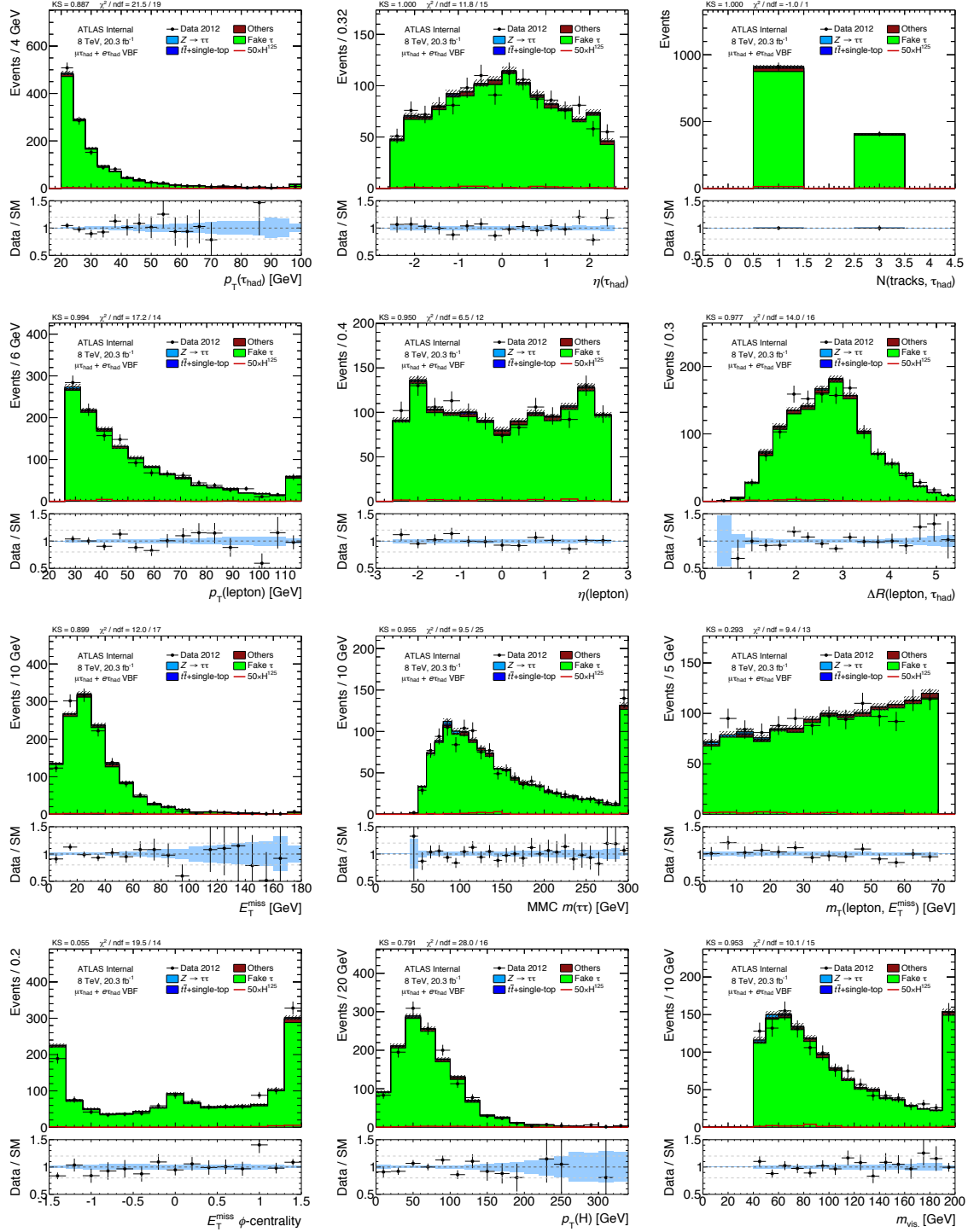


Figure A.1: Comparison of data and $j \rightarrow \tau_{\text{had}}$ prediction in the same sign CR for various event kinematics. Only statistical uncertainties are shown.

A. CONTROL REGIONS FOR FAKES

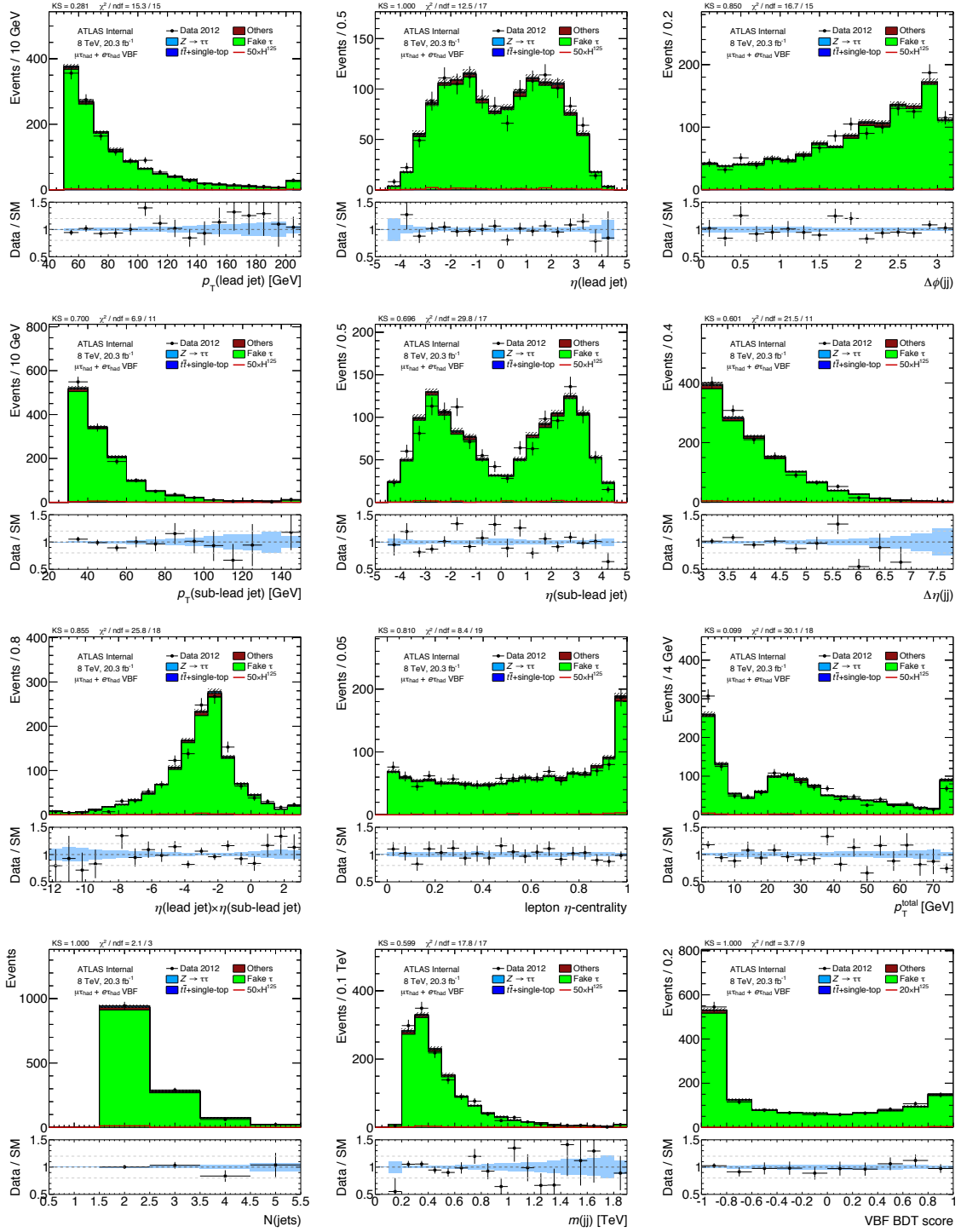


Figure A.2: Comparison of data and $j \rightarrow \tau_{\text{had}}$ prediction in the same sign CR for various event kinematics. Only statistical uncertainties are shown.

A. CONTROL REGIONS FOR FAKES

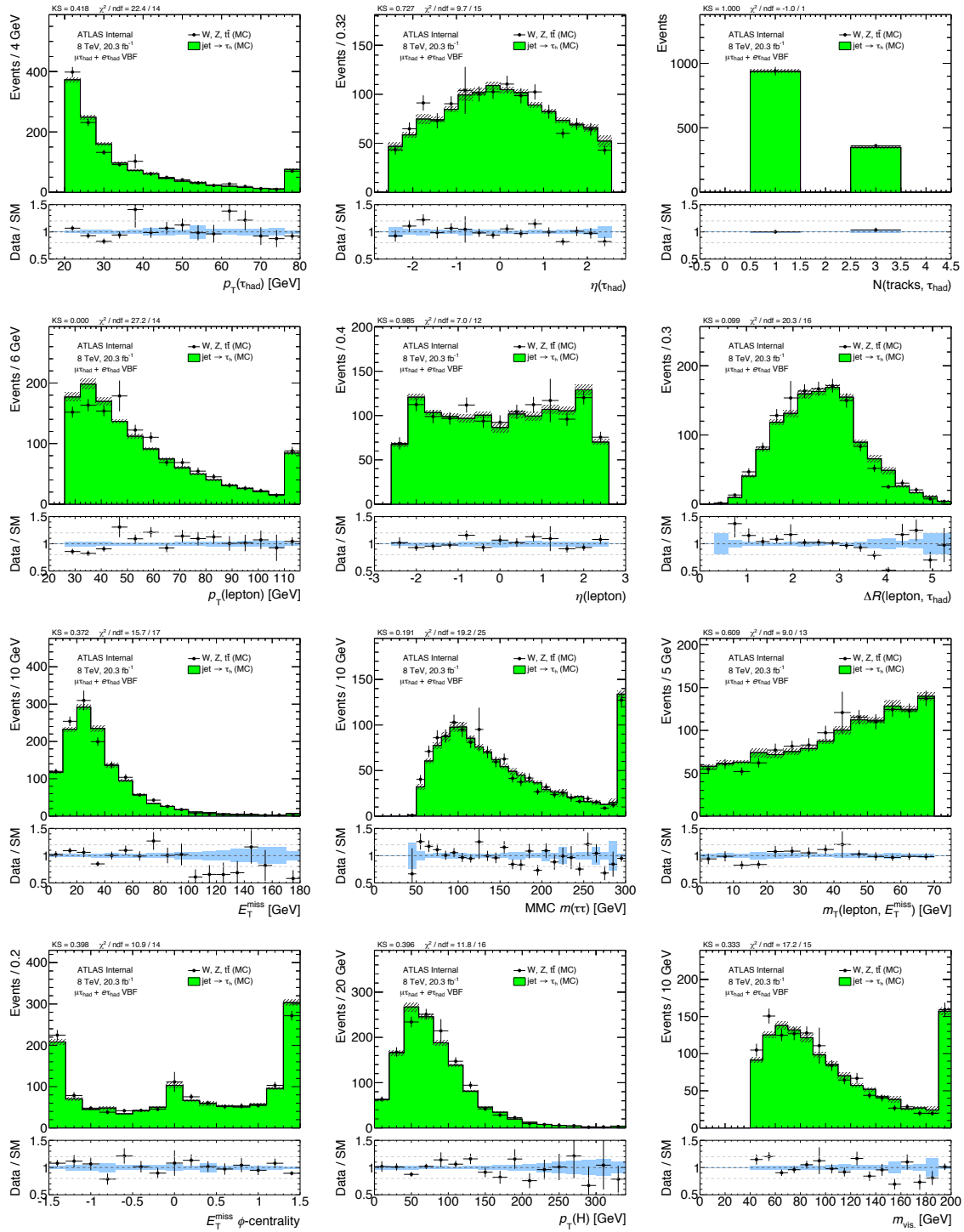


Figure A.3: Comparison of the prediction of identified taus and the $j \rightarrow \tau_{\text{had}}$ prediction, both in simulation, in the signal region for various event kinematics. Only statistical uncertainties are shown.

A. CONTROL REGIONS FOR FAKES

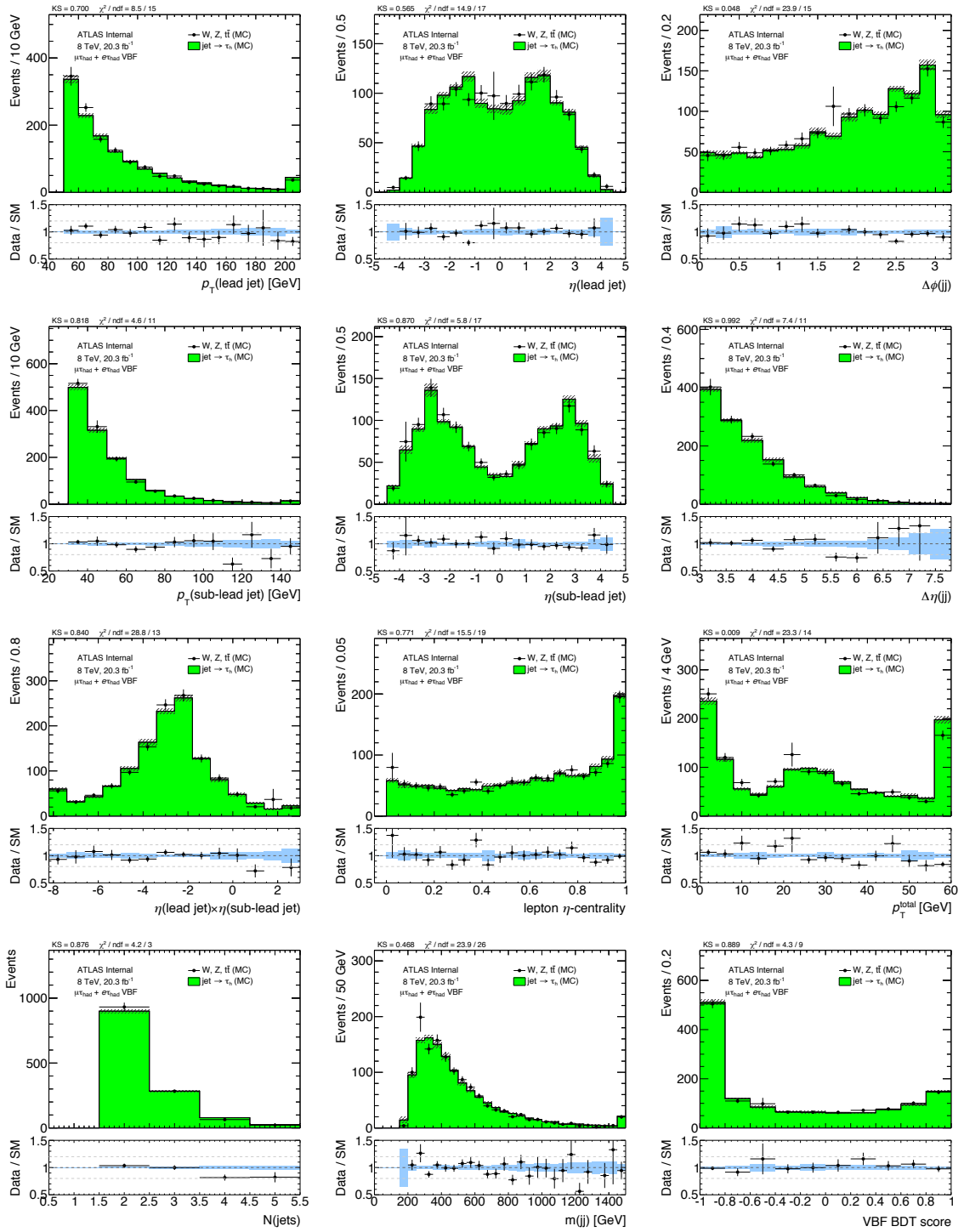


Figure A.4: Comparison of the prediction of identified taus and the $j \rightarrow \tau_{\text{had}}$ prediction, both in simulation, in the signal region for various event kinematics. Only statistical uncertainties are shown.

A. CONTROL REGIONS FOR FAKES

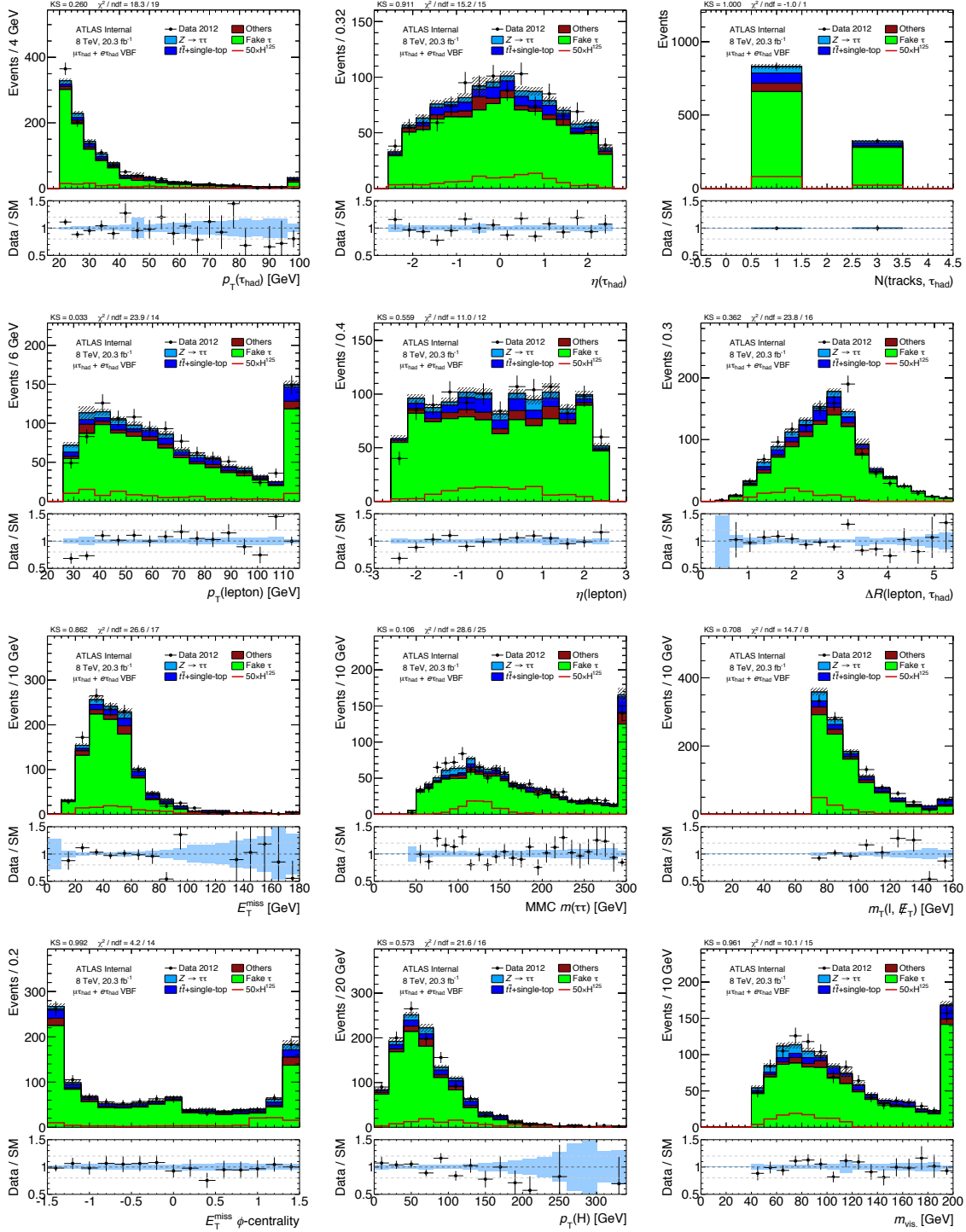


Figure A.5: Comparison of data and $j \rightarrow \tau_{\text{had}}$ prediction in the $W \rightarrow \ell\nu\ell$ CR for various event kinematics. Only statistical uncertainties are shown.

A. CONTROL REGIONS FOR FAKES

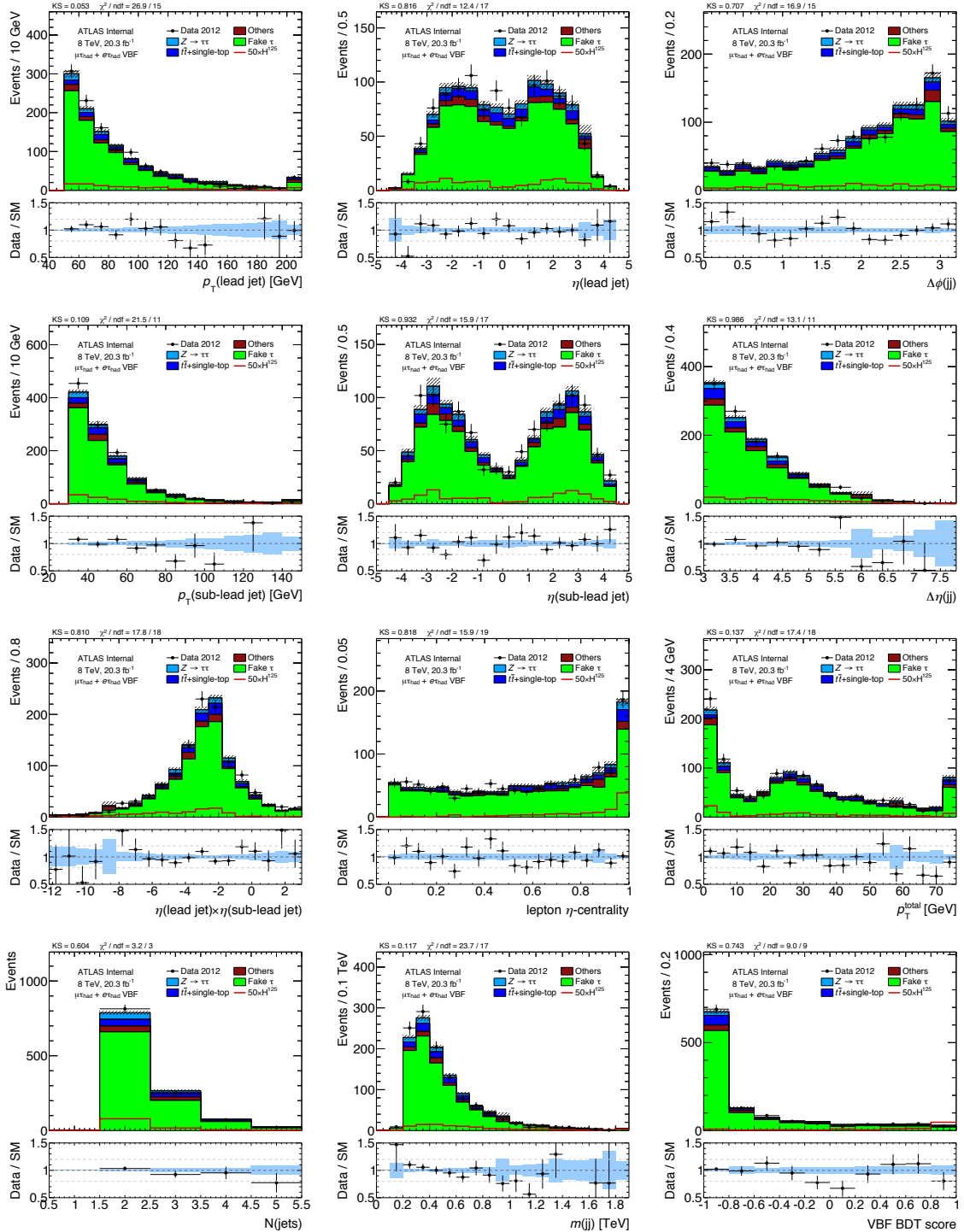


Figure A.6: Comparison of data and $j \rightarrow \tau_{\text{had}}$ prediction in the $W \rightarrow \ell\nu\ell$ CR for various event kinematics. Only statistical uncertainties are shown.

A. CONTROL REGIONS FOR FAKES

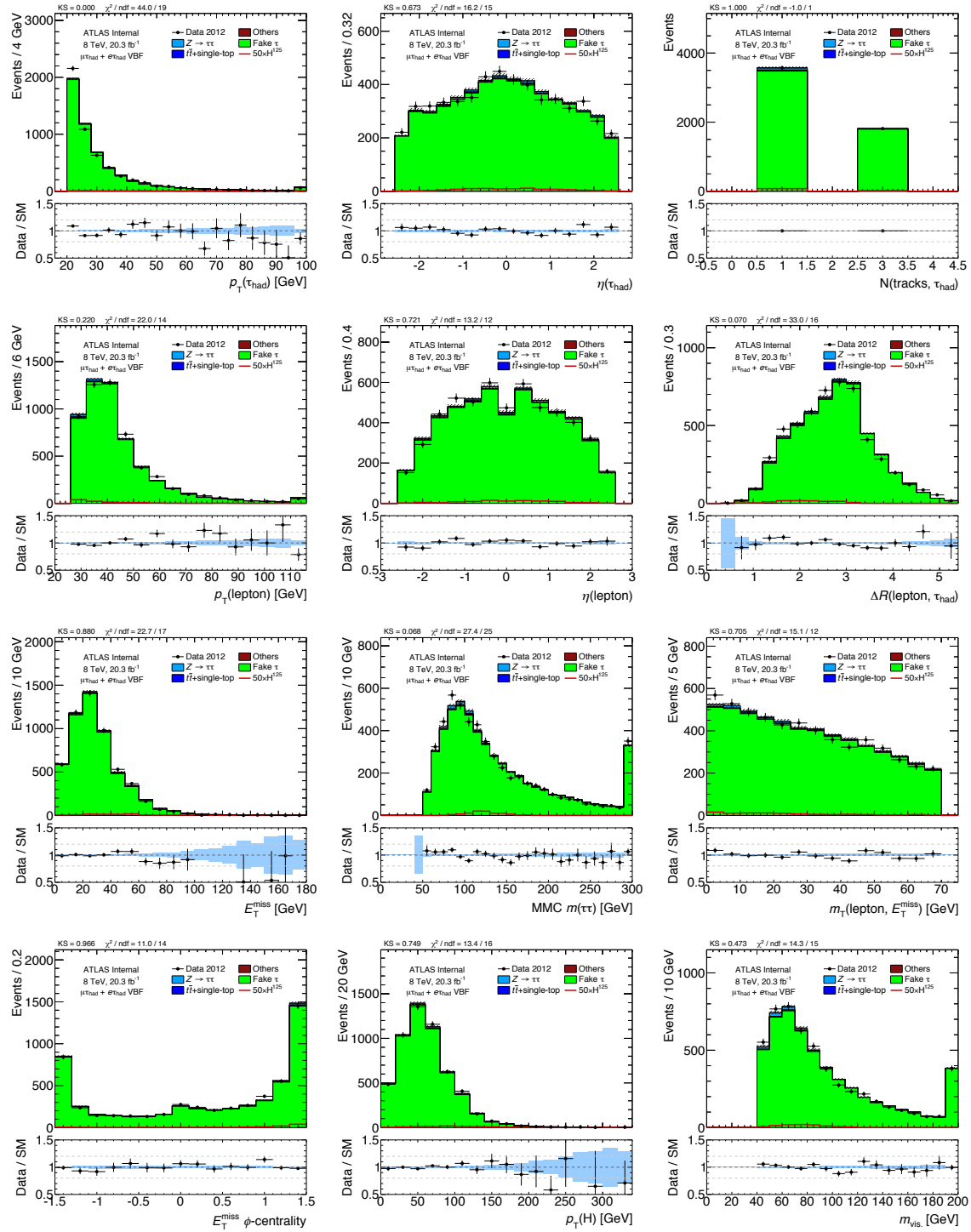


Figure A.7: Comparison of data and $j \rightarrow \tau_{\text{had}}$ prediction in the QCD CR for various event kinematics. Only statistical uncertainties are shown.

A. CONTROL REGIONS FOR FAKES

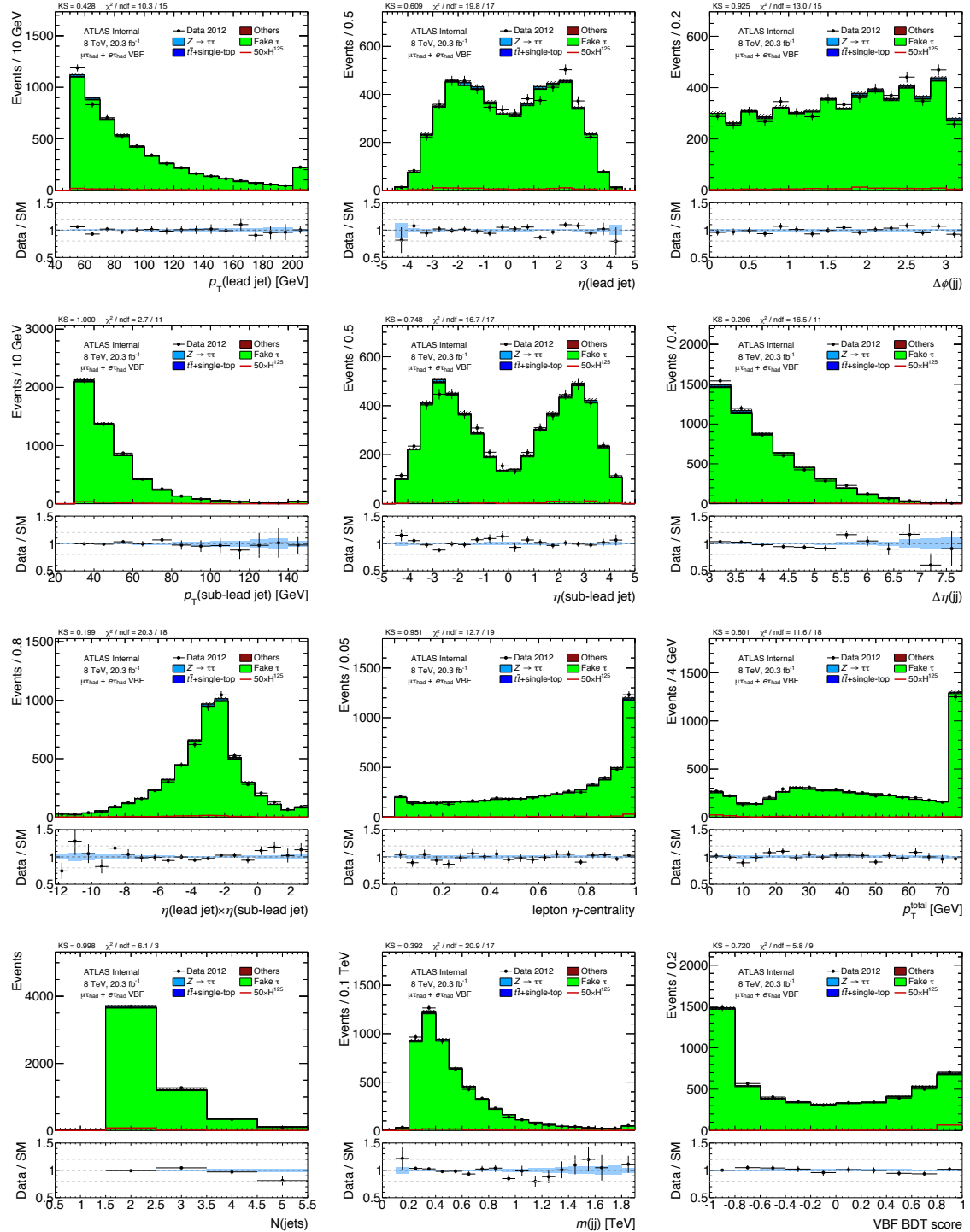


Figure A.8: Comparison of data and $j \rightarrow \tau_{\text{had}}$ prediction in the QCD CR for various event kinematics.
Only statistical uncertainties are shown.

A. CONTROL REGIONS FOR FAKES

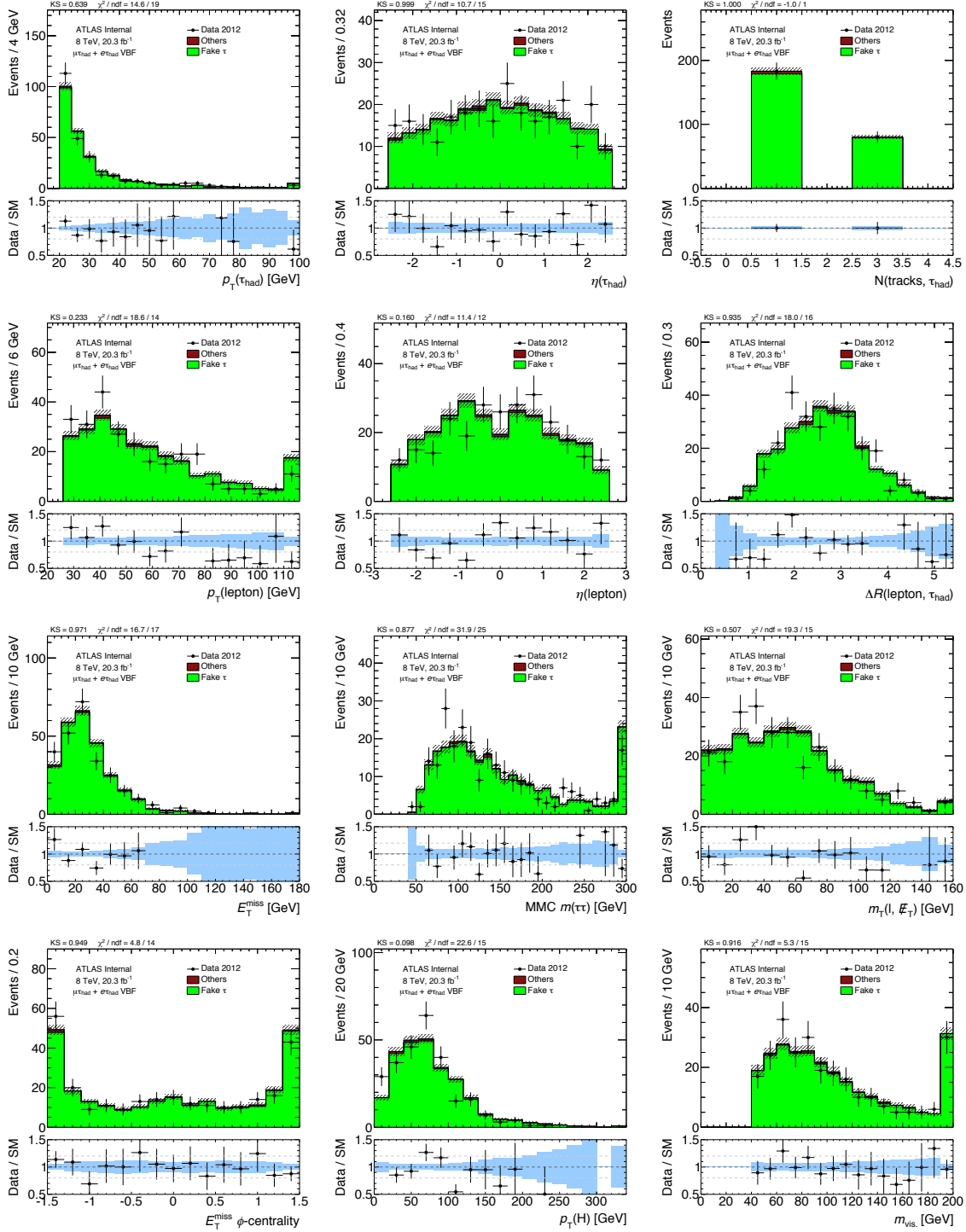


Figure A.9: Comparison of data and $j \rightarrow \tau_{\text{had}}$ prediction in the $Z \rightarrow \ell\ell$ CR for various event kinematics. Only statistical uncertainties are shown.

A. CONTROL REGIONS FOR FAKES

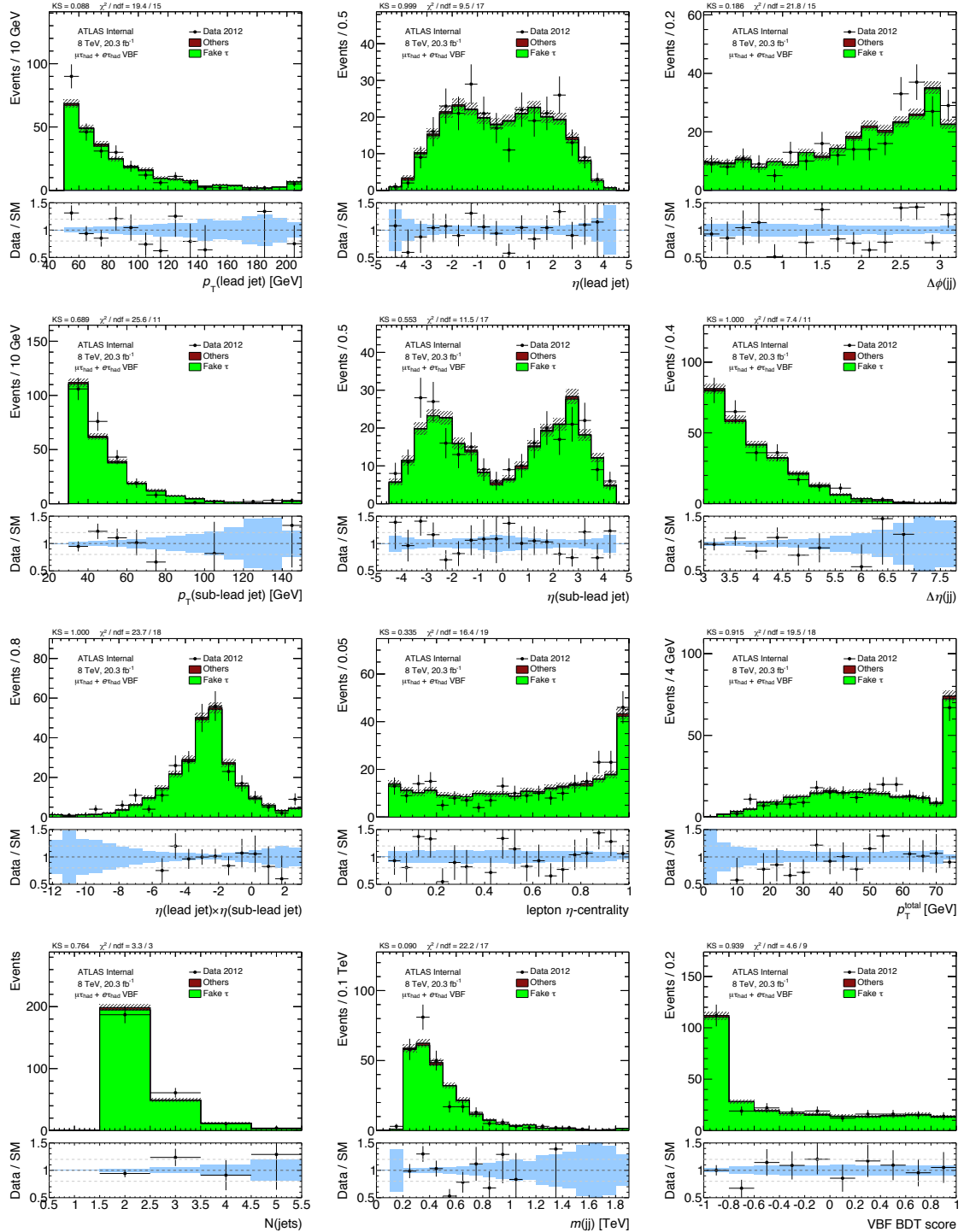


Figure A.10: Comparison of data and $j \rightarrow \tau_{\text{had}}$ prediction in the $Z \rightarrow \ell\ell$ CR for various event kinematics. Only statistical uncertainties are shown.

A. CONTROL REGIONS FOR FAKES

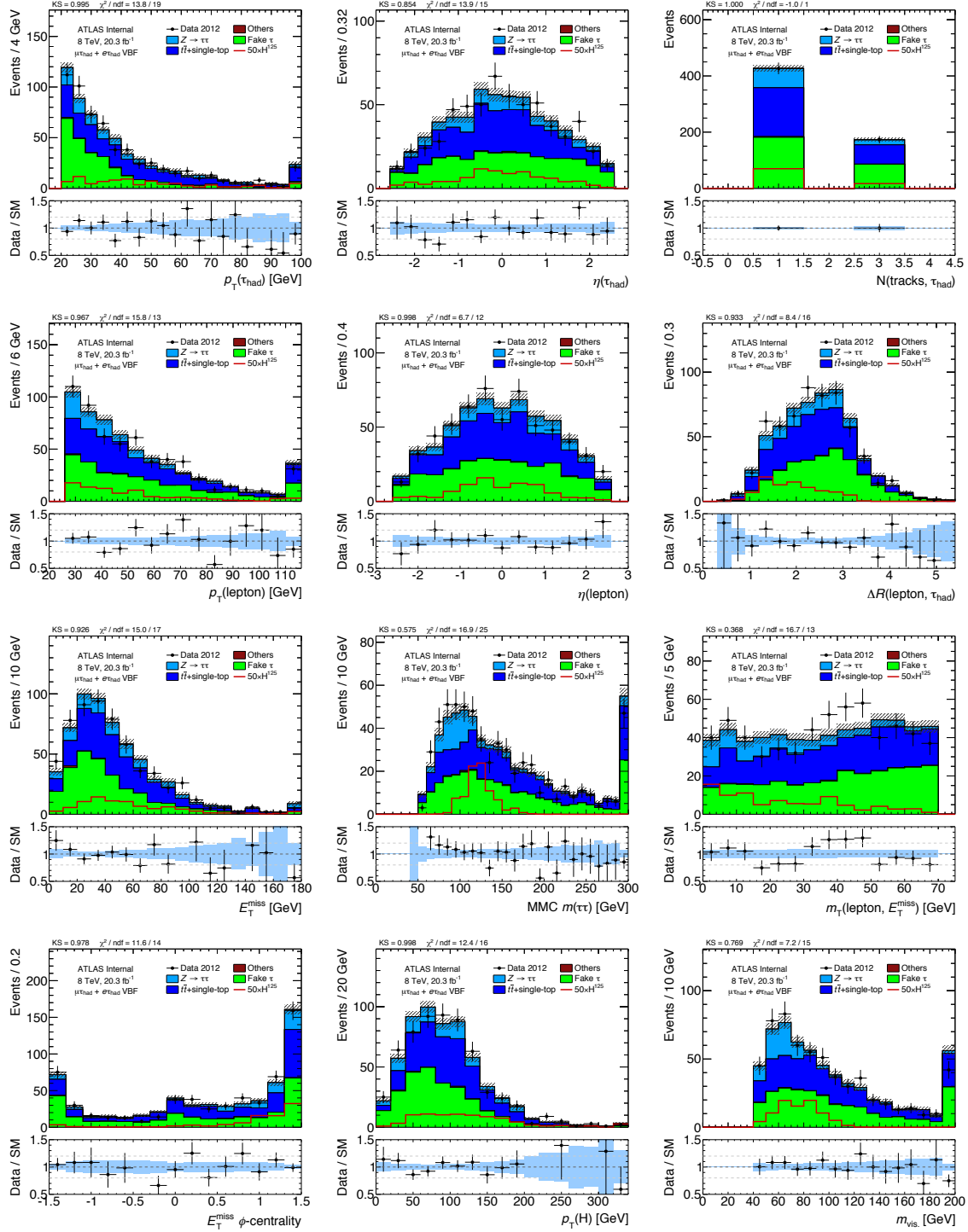


Figure A.11: Comparison of data and $j \rightarrow \tau_{had}$ prediction in the top CR for various event kinematics. Only statistical uncertainties are shown.

A. CONTROL REGIONS FOR FAKES

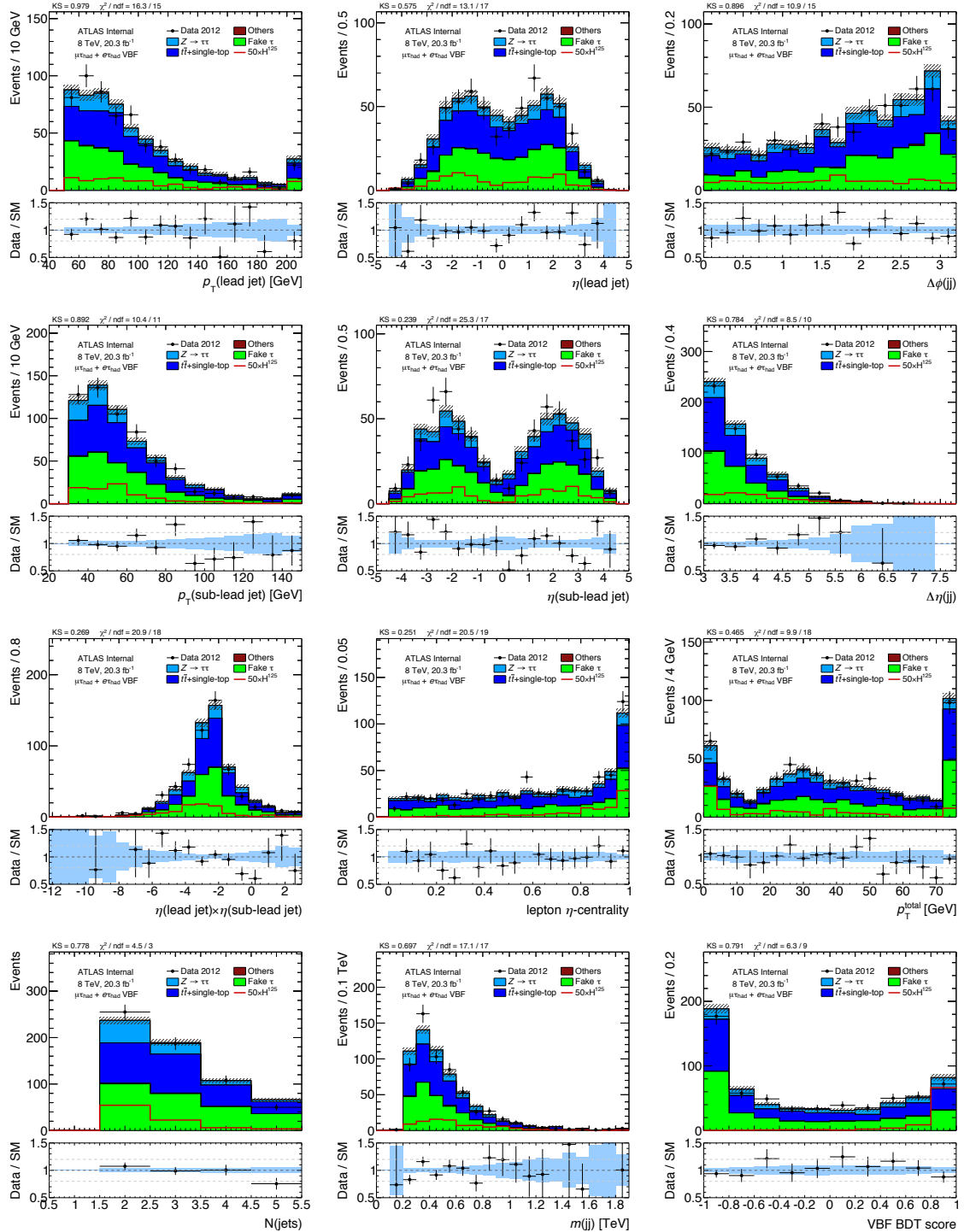


Figure A.12: Comparison of data and $j \rightarrow \tau_{\text{had}}$ prediction in the top CR for various event kinematics. Only statistical uncertainties are shown.

APPENDIX B

Inputs to the τ_{had} BDT identifier

Distributions of τ_{had} (signal) and QCD jets (background) for the BDT identification algorithm are shown.

B. INPUTS TO THE τ_{HAD} BDT IDENTIFIER

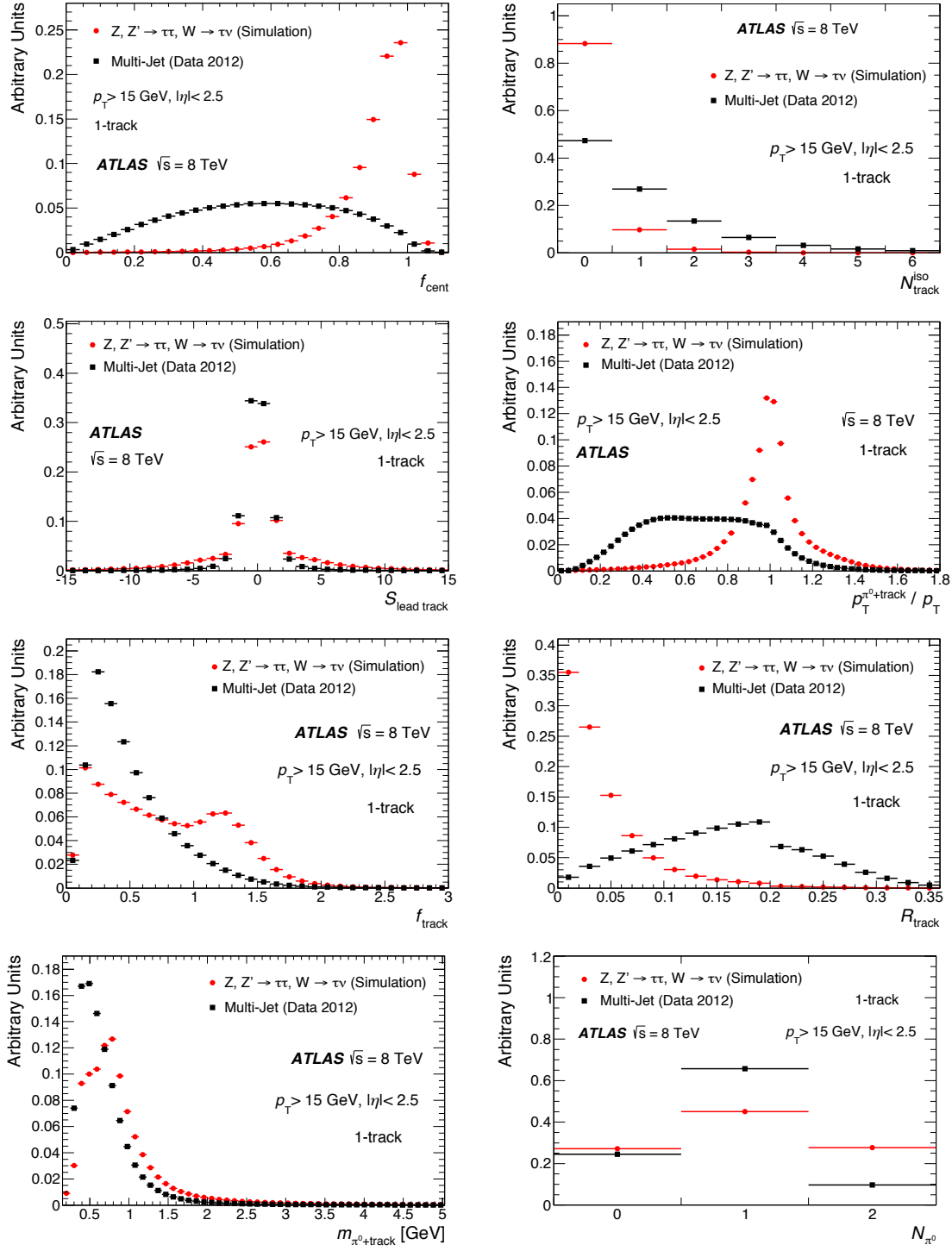


Figure B.1: Signal and background distributions for the full set of the discriminating variables in the 1-track τ_{had} jet discrimination algorithm [1].

B. INPUTS TO THE τ_{had} BDT IDENTIFIER

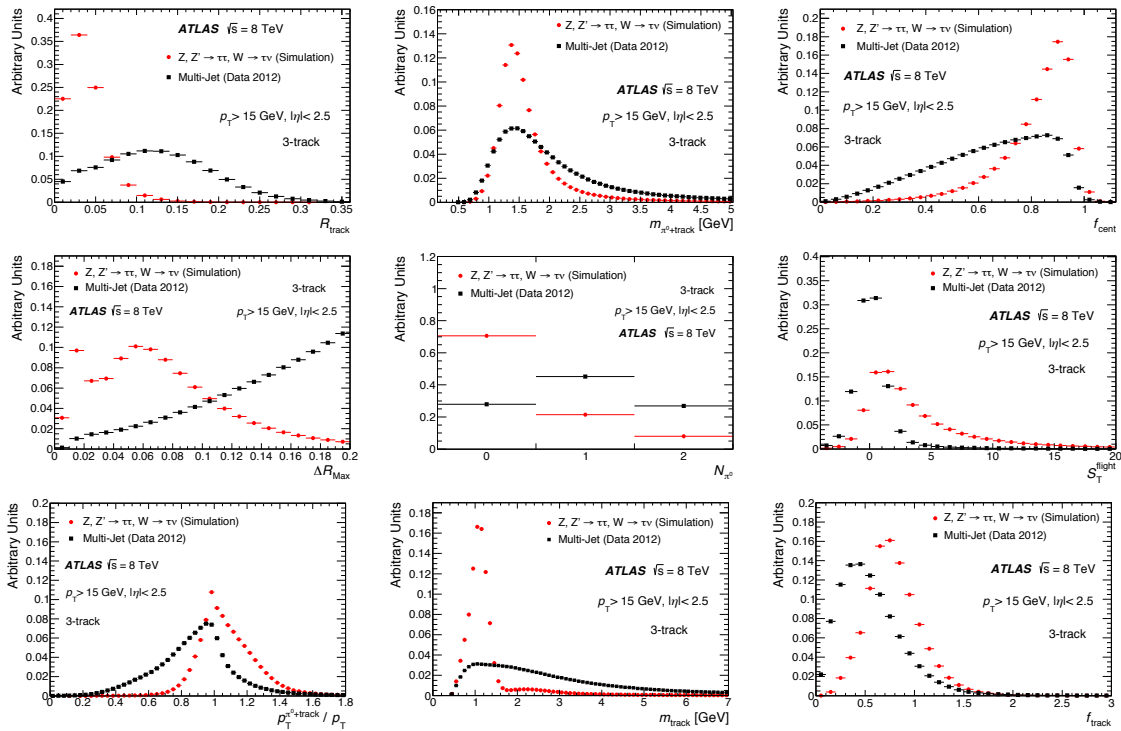


Figure B.2: Signal and background distributions for the full set of the discriminating variables in the 3-track τ_{had} jet discrimination algorithm [1].

APPENDIX C

Performance of $m_{\tau\tau}$ algorithms

Performance of various $m_{\tau\tau}$ reconstruction algorithms are shown. These are inputs to Section 5.5.

C. PERFORMANCE OF $m_{\tau\tau}$ ALGORITHMS

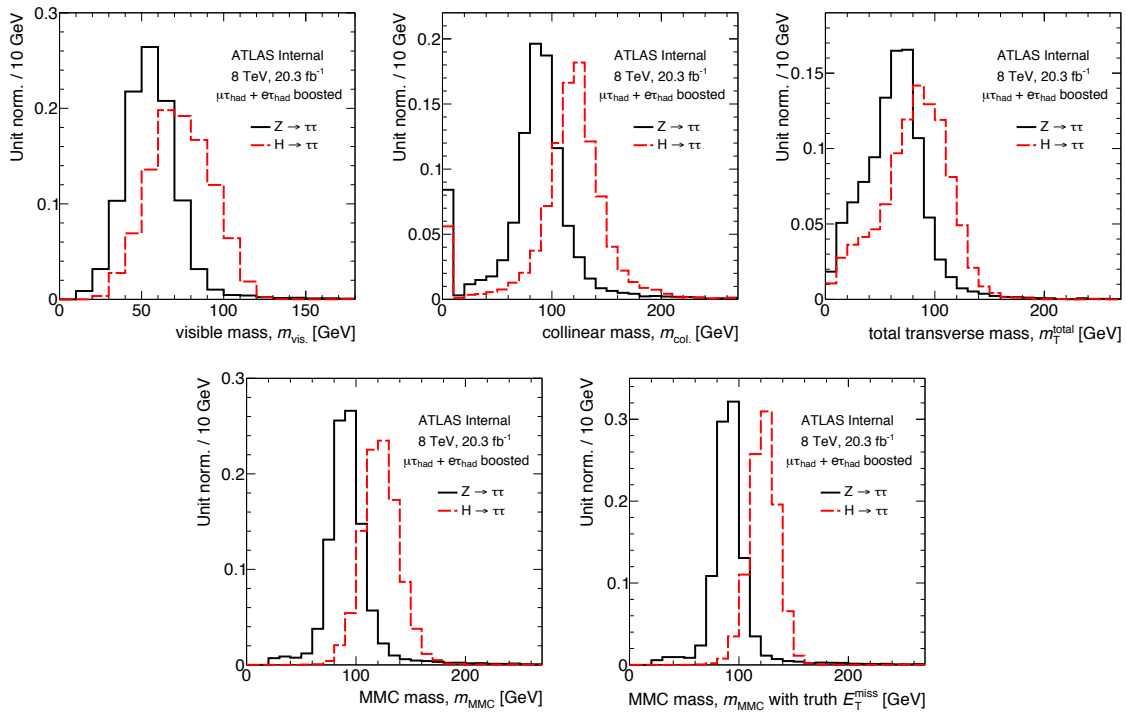


Figure C.1: Simulated predictions of $m_{Z \rightarrow \tau\ell\tau_{\text{had}}}$ and $m_{H \rightarrow \tau\ell\tau_{\text{had}}}$ in the boosted category for various $m_{\tau\tau}$ reconstruction algorithms.

C. PERFORMANCE OF $m_{\tau\tau}$ ALGORITHMS

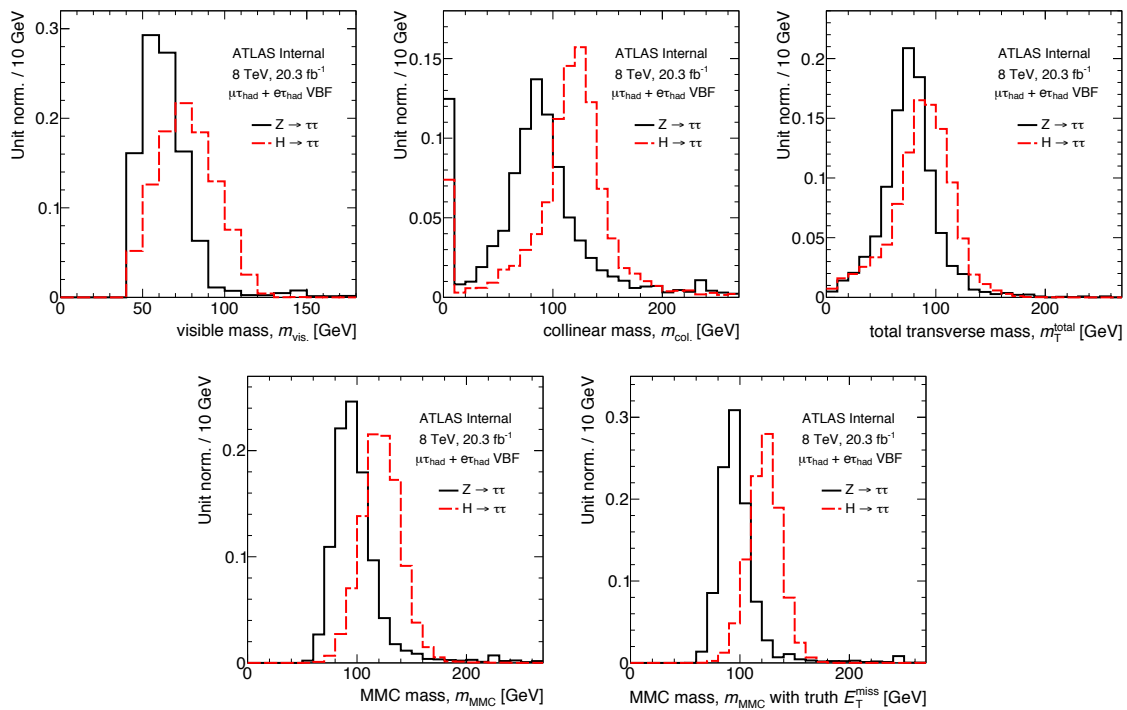


Figure C.2: Simulated predictions of $m_{Z \rightarrow \tau\ell\tau_{\text{had}}}$ and $m_{H \rightarrow \tau\ell\tau_{\text{had}}}$ in the VBF category for various $m_{\tau\tau}$ reconstruction algorithms.